



Aalborg Universitet

AALBORG UNIVERSITY  
DENMARK

## A Novel Multiple Correction Approach for Fast Open Circuit Voltage Prediction of Lithium-ion Battery

Jinhao, Meng; Stroe, Daniel-Ioan; Ricco, Mattia; Guangzhao, Luo; Maciej, Swierczynski; Teodorescu, Remus

*Published in:*  
I E E Transactions on Energy Conversion

*DOI (link to publication from Publisher):*  
[10.1109/TEC.2018.2880561](https://doi.org/10.1109/TEC.2018.2880561)

*Publication date:*  
2019

*Document Version*  
Accepted author manuscript, peer reviewed version

[Link to publication from Aalborg University](#)

*Citation for published version (APA):*

Jinhao, M., Stroe, D.-I., Ricco, M., Guangzhao, L., Maciej, S., & Teodorescu, R. (2019). A Novel Multiple Correction Approach for Fast Open Circuit Voltage Prediction of Lithium-ion Battery. *I E E Transactions on Energy Conversion*, 34(2), 1115-1123. Article 8528545. <https://doi.org/10.1109/TEC.2018.2880561>

### General rights

Copyright and moral rights for the publications made accessible in the public portal are retained by the authors and/or other copyright owners and it is a condition of accessing publications that users recognise and abide by the legal requirements associated with these rights.

- Users may download and print one copy of any publication from the public portal for the purpose of private study or research.
- You may not further distribute the material or use it for any profit-making activity or commercial gain
- You may freely distribute the URL identifying the publication in the public portal -

### Take down policy

If you believe that this document breaches copyright please contact us at [vbn@aub.aau.dk](mailto:vbn@aub.aau.dk) providing details, and we will remove access to the work immediately and investigate your claim.

# A Novel Multiple Correction Approach for Fast Open Circuit Voltage Prediction of Lithium-ion Battery

Jinhao Meng, *Student Member, IEEE*, Daniel-Ioan Stroe, *Member, IEEE*, Mattia Ricco, *Member, IEEE*, Guangzhao Luo, *Member, IEEE*, Maciej Swierczynski, *Member, IEEE*, Remus Teodorescu, *Fellow, IEEE*

**Abstract**—This paper proposes a novel fast open circuit voltage prediction approach for Lithium-ion battery, which is potential to facilitate a convenient battery modeling and states estimation in the energy storage system. Open circuit voltage measurement suffers from a long relaxation time (several hours, even days) to reach the thermodynamic equilibrium of the battery. On the basis of the feedback control theory, the proposed multiple correction approach utilizes the constrained nonlinear optimization of the power function in each curve fitting step. The voltage measurement in a short period is divided into several segments to correct the voltage prediction multiple times with the feedback errors after each curve fitting. The similarity between the shape of the power function and the variation of the terminal voltage during the relaxation time is utilized. The proposed method can speed up the time-consuming open circuit voltage measurement and predict the open circuit voltage with high accuracy. Experimental tests on a LiFePO<sub>4</sub> battery prove the validation and effectiveness of the proposed method in accurately predicting the open circuit voltage within a very short relaxation time (less than 15 min).

**Index Terms**—Open circuit voltage, multiple correction approach, fast prediction, lithium-ion battery.

## I. INTRODUCTION

LITHIUM-ION (Li-ion) batteries have recently become a promising energy storage component in various applications (e.g., Electric Vehicles (EVs) and Battery Energy Storage System (BESS)), due to their excellent performance [1]–[5]. Open Circuit Voltage (OCV) is related to the natural properties of a Li-ion battery, which is determined by the Gibbs energy in the electrochemical reactions. Accurate knowledge (measurement or estimation) of the OCV is necessary for different purposes: battery modeling [6]–[8], State of Charge (SOC) [9]–[11] and State of Health (SOH) [9], [12]–[14]

This work was supported in part by the Key Program for International S&T Cooperation and Exchange Projects of Shaanxi Province under Grant 2017KW-ZD-05, and in part by the Fundamental Research Funds for Central Universities under Grant 3102017JC06004 and Grant 3102017OQD029. (Corresponding author: Guangzhao Luo, phone: 0086-029-88431335; fax: 0086-029-88431310; e-mail: guangzhao.luo@nwpu.edu.cn)

J. Meng and G. Luo are with School of Automation, Northwestern Polytechnical University, Xi'an 710072, China (e-mails: scmjh2008@163.com; guangzhao.luo@nwpu.edu.cn)

D.-I. Stroe, M. Ricco and R. Teodorescu are with the Department of Energy Technology, Aalborg University, Aalborg 9220, Denmark (e-mails: dis@et.aau.dk; mri@et.aau.dk; ret@et.aau.dk).

M. Swierczynski is with Lithium Balance A/S, Smørum 2765, Denmark (e-mail: mas@lithiumbalance.com).

estimation, and also the evaluation of cell-to-cell variation in the battery pack [15].

As an indicator of the available energy in a battery, SOC cannot be directly measured by sensors. OCV can estimate the SOC on the basis of an established OCV-SOC function beforehand. However, Li-ion batteries, especially the LiFePO<sub>4</sub> (LFP) chemistry, is characterized by a relatively flat OCV-SOC curve [16]. An accurate OCV measurement is then needed to ensure a precise SOC estimation of the LFP battery. The behavior of the OCV-SOC curve is illustrated for example in [17], [18], where the OCV variation in the 30%–80% SOC range is only 72 mV. Furthermore, OCV contains information regarding the capacity loss, which can be further used for SOH estimation. For example, Roscher et. al. investigated the capacity fade of a high-power LFP battery by continuously cycling the battery with 5C current rate over a period of 3000 cycles [19]; they showed that OCV corresponding to the high SOC area was able to reveal information of the capacity fade. Chen et. al. in [20] tested a Sanyo UR18650W 1.5Ah Li-ion battery with 1000 cycles, and the OCV curve was reversed with more cycles applied. The OCV was also used to quantify the variations of the cells in a battery pack and further helped enhancing the balancing strategy in the Battery Management System (BMS) [15]. Moreover, OCV is crucial for the battery dynamical modeling. In a lumped Equivalent Circuit Model (ECM), the only correlation between the battery terminal voltage and the SOC is the OCV-SOC function [21]–[23]. For this reason, an accurate OCV measurement is extremely desirable. In addition, the accuracy of the model-based SOC estimation is also affected by the established OCV-SOC function in the battery performance model.

There are typically three different ways to obtain the OCV. In order to measure an accurate OCV in the laboratory, the battery has to rest several hours or even days before reaching its inner equilibrium [17], [24], [25]. “Quasi” OCV measurement is an alternative approach to determine the OCV by charging and discharging the battery with a very low current rate [26]. Due to the time efficiency, many researchers consider the OCV obtained as the average voltage between charging and discharging condition [24], [27]. The foregoing two methods are time-consuming, while using the average voltage as the OCV has the least accuracy among them. Accurate OCV measurement is very time-consuming because the diffusion of

the Li-ion inside the battery is a process with very slow dynamics. Fortunately, there are always some interruptions during the working condition of the battery. For example, EVs are frequently stopped in a traffic jam or at the traffic light, and they are also parked somewhere when their owners do not need them. However, the current interruptions in those conditions are usually too short to measure an accurate OCV by traditional methods. More information about the battery status can be obtained to improve the performance of the applications, if an accurate OCV is obtained during the short interruption. OCV measurement in the energy storage applications is meaningful and challenging, and fast OCV prediction is a potentially alternative solution.

Some approaches have already been considered to reduce the time requirements of the OCV measurement. OCV physical models are based on the thermodynamic characteristics in the positive and negative electrodes of the battery [28], [29]. OCV in each electrode is represented by the functions of its utilization in those physical models [30]. A number of microscopic parameters are essential to model the battery's external characteristics in this case. Those parameters are impossible to be identified from the commercial datasheet, which means that the dedicated destructive measurements have to be performed. Additionally, this kind of models also suffers from a large amount of computing burden [31]. ECMs can intuitively interpret the battery characteristics in a simple way [32], [33]. The resistance and capacitance components in the ECM usually have their own physical meanings. Moreover, the parameters in ECM are much easier to be obtained from the current pulse test or by the online parameter identification methods [6], [34], [35]. This is the reason why ECMs are also a popular choice for the OCV prediction [36]–[38]. However, one drawback of ECM based OCV prediction is that once the ECM is determined, the accuracy of the prediction is limited by the fixed structure and the parameters [39]. From an engineering point of view, it is better to predict OCV rapidly without any prior knowledge of the battery electrochemistry. In order to utilize the voltage characteristics during the relaxation time, curve fitting based methods are applied to predict the battery OCV [40], [41]. The voltage measurement in a very short relaxation time is used to predict the battery voltage after a long term current interruption. However, most OCV prediction methods rely on a constant expression and use the measurement data only once or twice in their curve fitting [36], [37], which restrains the prediction accuracy.

In this paper, a novel OCV prediction method using a multiple correction approach is proposed. The benefits are that the proposed method not only improves the time efficiency of the OCV measurement in the laboratory but also has the potential ability to accurately predict the OCV during a short battery idling interval in real applications. Additionally, the proposed method does not rely on any previous electrochemical knowledge of the battery. Deep analyzing the measurement may help to fully understand the information hidden behind those data. After investigating the features of the terminal voltage, the measurement during a very short relaxation time is used to fit the preliminary curve. Then, the errors of the first

curve are calculated in the next correction window and are feedback to form the input of the next curve fitting. With several correcting processes, the accuracy of the OCV prediction is gradually improved. In order to utilize the shape of the voltage, the curve fitting is transformed into a constrained nonlinear optimization problem. Hence, the proposed multiple correction approach relies on solving a series of the constrained nonlinear optimization problems. The proposed method is capable of predicting the OCV of LFP battery rapidly and accurately.

This paper is organized as follows. The features of the terminal voltage during the relaxation time are analyzed in Section II. A novel multiple correction approach for fast OCV prediction is detailed in Section III. Section IV presents the experimental validation of the proposed method. The conclusions are summarized in Section V.

## II. TERMINAL VOLTAGE DURING THE LI-ION BATTERY RELAXATION TIME

OCV represents the difference between the electrodes' potentials when there is no current flow through the battery. Therefore, OCV has to be measured in the no-load condition after a long relaxation time that allows the cell to reach the thermodynamic stability. Equation (1) and (2) are the ways to express the relationship between the terminal voltage and the OCV. The voltage due to the ohmic resistance disappears immediately after the current is cutoff. However, the voltage caused by the polarization resistance requires an extremely long relaxation time.

$$U_t = \text{OCV} - I \times (R_\Omega + R_p) \quad (1)$$

$$U_t = \text{OCV} - \eta_+ - \eta_- - I \times R_\Omega \quad (2)$$

where  $\eta_+$  is the over potential in the anode,  $\eta_-$  is the over potential in the cathode,  $U_t$  is the terminal voltage,  $R_p$  is the polarization resistance,  $R_\Omega$  is the ohmic resistance, and  $I$  is the current.

### A. OCV Measurement and Battery Relaxation Time

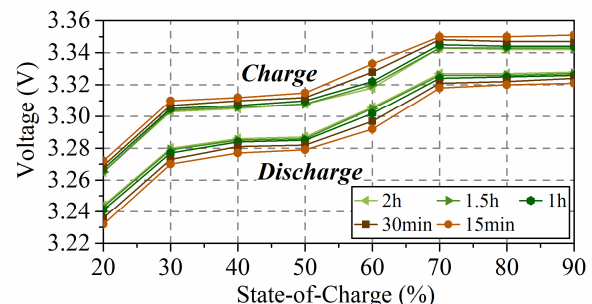


Fig. 1. OCV-SOC curves with different relaxation time

Fig. 1 shows how the OCV of a LFP battery changes when measured with different relaxation times (15 min, 30 min, 1 hour, 1.5 hours, 2 hours). With a longer relaxation time, the OCV measurement in the charging and discharging condition are getting closer to each other. The OCV values increase with longer relaxation time in the discharging process, while it

decreases in the charging condition. Since the variation of the voltage during the battery idling is a slow process, accurate OCV-SOC curve always needs a very long time. The rough OCV measurement decreases the value of OCV in real applications, which indicates that accurate OCV prediction in a short relaxation time is of great importance.

### B. Battery Voltage in the Long Relaxation Time Area

In order to fully understand the features of the terminal voltage during the relaxation time, a LFP battery is rest for 24 hours after charging. The variation of the OCV is recorded in Fig. 2.

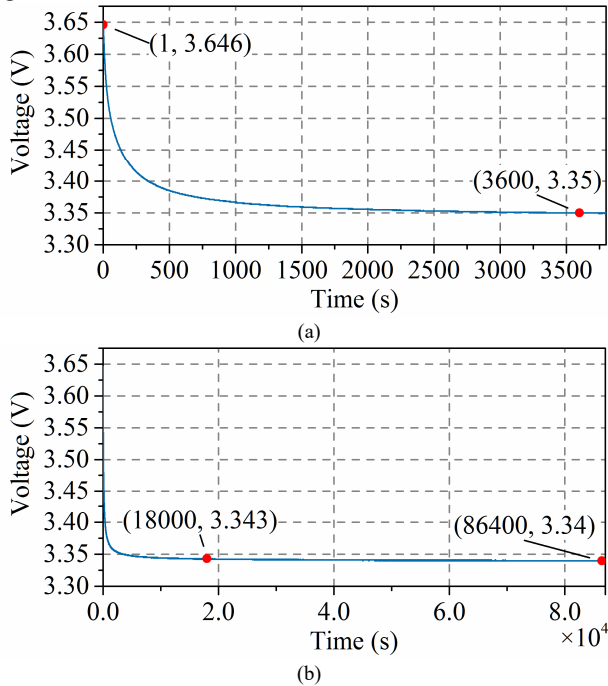


Fig. 2. Terminal voltage variation after charging the battery to 100% SOC: (a) 1 hour's relaxation time; (b) 24 hours' relaxation time.

The voltage falls down faster at the beginning of the relaxation (Fig. 2(a)), and the decreasing rate becomes slower with a longer relaxation time (Fig. 2(b)). It is clearly seen in Fig. 2(b) that the voltage decreases less than 3 mV from 5 hours to 24 hours of relaxation, but almost 296 mV in the first relaxation hour. Therefore, the voltage deviation from 5 to 24 hours is further used as the constraint of the curve fitting, which helps improving the accuracy of OCV prediction. In other words, if the variation of the voltage is constrained to less than 3 mV after 5 hours in Fig. 2, the curve fitting results will close to the voltage measurement in the same area. Utilizing the additional information from the voltage measurement, an improved OCV prediction is expected.

### III. FAST OCV PREDICTION APPROACH

Utilizing the voltage characteristics of the battery during the relaxation time, a novel multiple correction approach for fast OCV prediction is proposed in Section. III. A power function has been used to describe many natural phenomena [42]. Considering the shape of the voltage during the relaxation time,

this paper chooses the power function to depict the battery voltage and predict the OCV. The following power function is used,

$$y = f(t) = k_1 \cdot t^{k_2} + k_3 \quad (3)$$

where  $k_1$ ,  $k_2$  and  $k_3$  are the parameters,  $t$  is the relaxation time.

#### A. Directly Curve Fitting (DCF)

In order to explain the reason why we propose this fast OCV prediction method, the terminal voltage measured at 100% SOC after charging condition is used as an example. Fig. 3(a) shows the voltage prediction results by fitting (3) with different length of the measurement. In Fig. 3(a),  $U$  is the voltage measurement from sensors and Ref. is the voltage at 24 hours. The measured voltage during the relaxation time of 10 minutes, 30 minutes, 1 hour, 2 hours, 5 hours, and 10 hours are used to calculate the parameters in (3). With more data added to the curve fitting, the predicted voltage is closer to the measurement and the OCV prediction is more accurate. However, as seen from the enlarged figure in Fig. 3(a), there is still a clear deviation between the OCV prediction and the reference even using the data during 2 hours' relaxation time. The OCV prediction is 3.3359 V if the measured voltage during 10 hours' relaxation period is adopted. By comparing with the reference, the estimation error is still 4.2 mV.

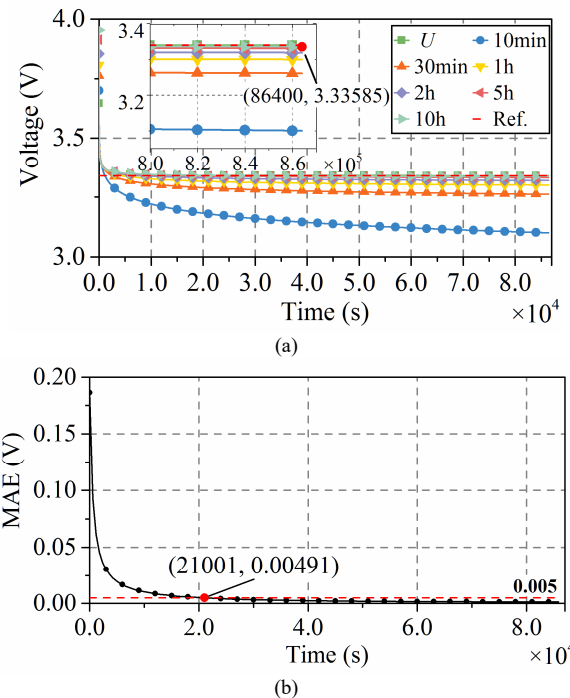


Fig. 3. The voltage prediction of DCF: (a) results; (b) MAE.

In Fig. 3(a), the accuracy of OCV prediction is related to the length of the dataset used for curve fitting. It is necessary to analyze the relationship between them, in order to use the voltage measurement in a more effective way. The measurement is increased with 10 minutes' interval to demonstrate how the accuracy of the voltage prediction changes with the length of the dataset. The variation of the Mean Absolute Error (MAE) for the voltage prediction is shown in Fig. 3(b).

$$MAE = \frac{1}{N} \sum_{t=1}^N |f(t) - y_t| \quad (4)$$

where  $f(t)$  is the predicted voltage and  $y_t$  is the measurement from sensor.

The MAE reduces extremely fast in the initial stage but becomes slower after 3 hours, which indicates the limitation of DCF on describing the battery voltage.

### B. Curve Fitting with Constraint (CFC)

In order to improve the ability of (3) on describing the battery voltage behavior in the resting period, the features of the voltage are further utilized as a constraint to the curve fitting. Subsequently, the curve fitting is transferred into a constrained nonlinear optimization problem, which is described as follows:

$$\text{Minimize } g(k_1, k_2, k_3) = \sum_{t=1}^N (f(t) - y_t)^2, t=1, \dots, N \quad (5)$$

$$\text{Subject to } |f(t_1) - f(t_2)| \leq \Delta U_{\text{limit}}, 1 \leq t_1 \leq N, t_1 < t_2 \leq N \quad (6)$$

where  $f(t)$  and  $y_t$  are the same as in (3),  $t$  is the relaxation time,  $t_1$  and  $t_2$  are the time intervals which employ the constraints on the voltage variation,  $\Delta U_{\text{limit}}$  is defined as the voltage limitation between  $t_1$  and  $t_2$ . In the above equations, (5) guarantees the accuracy of the curve fitting, (6) constrains the predicted voltage especially in the slow variation region approaching the measurement. Generally,  $\Delta U_{\text{limit}}$  is set to a small value to make full use of the voltage variation after a long relaxation time.

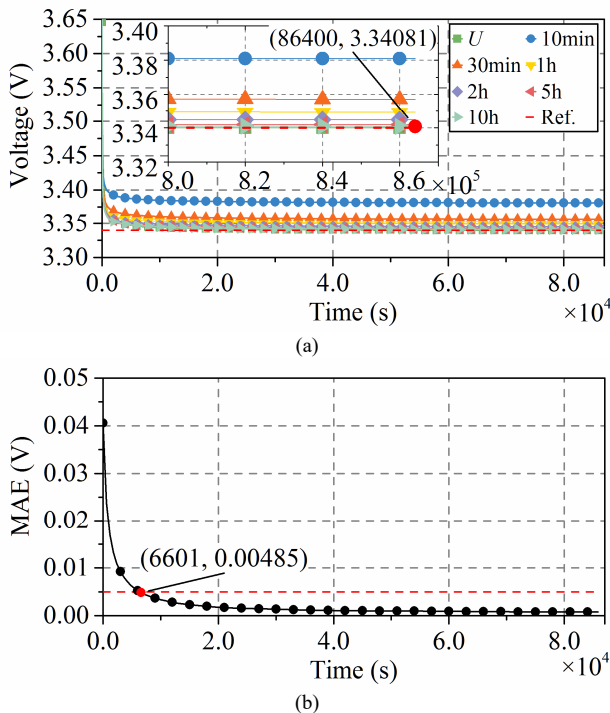


Fig. 4. The voltage prediction of CFC: (a) results; (b) MAE.

As a comparison to the results in Fig. 3(a), the same length of measurement is also used to solve the constrained nonlinear optimization in (5) and (6). The predicted voltage with CFC is much closer to the measurement in Fig. 4(a). Additionally, the OCV prediction error using 10 hours' dataset is less than 1 mV. It is clear in Fig. 4(b) that the MAE of CFC decreases faster

than that of DCF. The MAE reaches the prediction error band ( $\leq 0.005$  V) in Fig. 4(b) (after 6601s), which is more than three times faster than that in Fig. 3(b) (after 21001s). A comparison between the results in Fig. 3(a) and Fig. 4(a) is listed in Table I. It is obvious from the absolute errors in Table I that the accuracy of OCV prediction is significantly improved by adding the constraint (6).

TABLE I

A comparison of the absolute errors in Fig. 3(a) and Fig. 4(a) (Unit: V)

Data length	Absolute error in DCF (Fig.3(a))	Absolute error in CFC (Fig.4(a))
10min	0.2394	0.0409
30min	0.0785	0.0171
1h	0.0400	0.0092
2h	0.0208	0.0047
5h	0.0086	0.0018
10h	0.0042	$8.1237 \times 10^{-4}$

### C. The Proposed Multiple Curve Fitting with Constraint (MCFC)

According to the previous results, it is still difficult to obtain an accurate OCV prediction in a short relaxation time. Since using the dataset once for curve fitting is similar to an open loop structure, a certain length of the measurement is chosen to calculate the final result. In order to utilize the measurement, a closed-loop structure is proposed with the basic idea from the feedback control. In MCFC, the dataset is divided into several groups. After the preliminary curve fitting using the first group, the errors between the voltage prediction and the measurement in the next group are feedback to form the input of the second curve fitting. The feedback mechanism of the curve fitting error continues until all the groups are traversed. With the benefit of the proposed structure, accurate OCV can be predicted in even shorter relaxation time. As shown in Fig. 5, the shape of the error is similar to the variation of the voltage curve in Fig. 2(b).

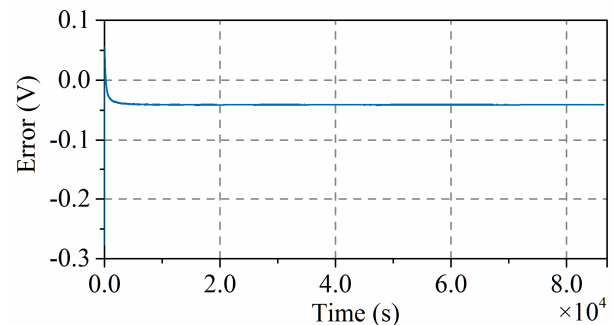


Fig. 5. Error of the constrained curve fitting results using the data in 10 minutes

The error drops extremely fast in the early stage and then the drop slows down with a longer relaxation time. Hence, (5) and (6) are possible to be used again after the first curve fitting. Since the voltage variations in different SOCs have some similarities, the proposed multiple correction can be used in both charging and discharging conditions.

The flowchart of the proposed multiple correction structure is shown in Fig. 6. The parameters related to the OCV prediction are the correction times  $M$ , the length of the first correction  $L_1$  and the length of the rest  $M-1$  corrections  $L_w$ .

After fitting the voltage with the initial  $L_1$  measurement, the preliminary function  $f_1(x)$  is obtained. The voltage prediction error is then calculated for the next constrained nonlinear optimization. Afterwards, the optimization processes repeat  $M-1$  times to predict the final OCV. It should be noted that the curve fitting is always constrained by (6) in each correction loop. Therefore, the predicted OCV is the sum of  $M$  times correction and the final prediction is expressed as,

$$OCV = \sum_{i=1}^M f_i(t) \quad (7)$$

where  $f_i(t)$  is the results of the  $i$ -th curve fitting.

The proposed multiple correction structure is capable of utilizing the features of the voltage curve in the long-term relaxation period and also the curve fitting error after each correction. In this way, the shape information of the voltage during the battery idling time is fully used for OCV prediction.

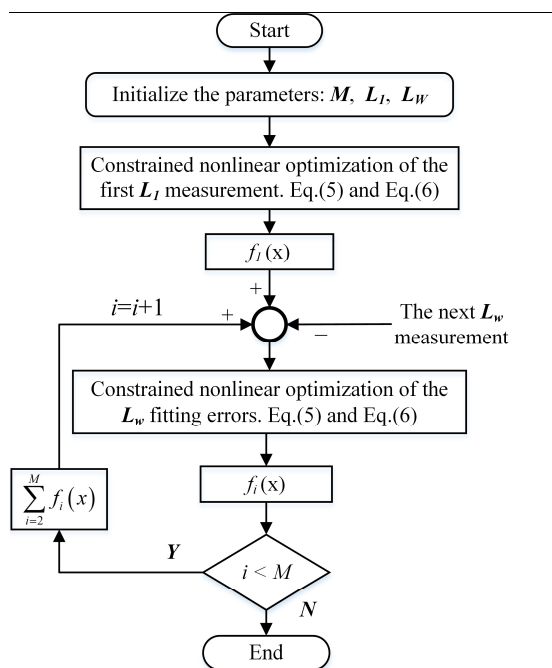


Fig. 6. The flowchart of the proposed multiple correction structure

#### IV. EXPERIMENTAL VALIDATION

In this section, the proposed structure is validated on a commercial LFP battery with the parameters listed in Table II.

TABLE II.

The datasheet of the LFP battery

Item	Rating
Nominal capacity	10 Ah
Nominal voltage	3.2 V
Nominal current	5 A (0.5C)
Maximum voltage	3.65 V
Cutoff voltage	2.0 V

The structure of the test bench is shown in Fig. 7, which

consists of a host computer, a battery test station, and a 10 Ah LFP battery. The test chamber is able to charge and discharge the battery with a predefined current profile, and control the ambient temperature during the test at the same time. The host computer collects the measurement from battery for the verification. The sample time is constantly set to 1 second and the ambient temperature is 25 °C for all the tests.

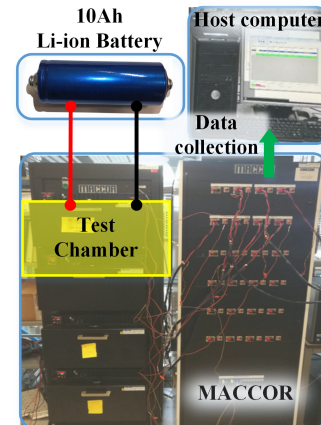


Fig. 7. Structure of the test bench

The schematic of the current waveform and the corresponding voltage is shown in Fig. 8, where the battery is charged or discharged to a certain SOC with the nominal current 5A in part A, and then the battery voltage in area B is collected to verify the proposed method.

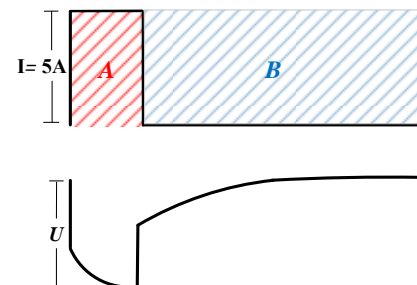


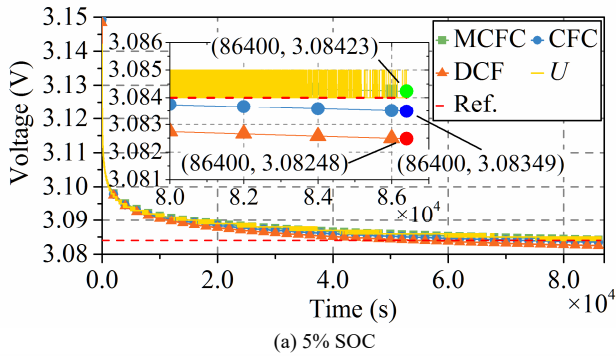
Fig. 8. The schematic of the current and voltage in the experimental test

#### A. Validation with Twenty-four Hours' Relaxation Time

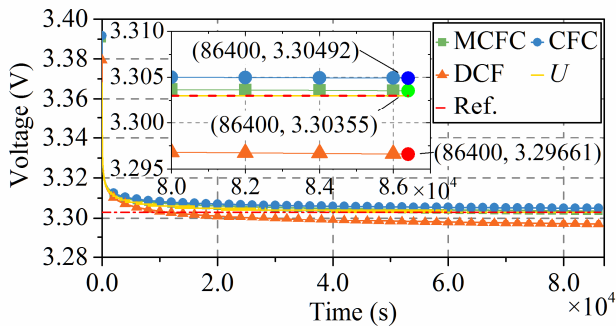
In order to verify the long-term performance of the proposed method, the LFP battery voltage is collected during 24 hours' relaxation time. Here we make the following definitions of the methods. DCF method simply fits the voltage curve with (3) for OCV prediction. CFC method solves the nonlinear constrained optimization of (5) and (6) once, while MCFC uses the proposed multiple correction structure in Fig. 6. It should be noted that all the methods are implemented with the same measurement to guarantee the fairness of the comparison. The terminal voltage during the first 15 minutes of the relaxation time is used to predict the OCV in this experiment. Among the three methods, DCF and CFC use the measured voltage directly. In MCFC,  $L_1$  is specially set to the measurement of the first 10 minutes.  $L_w$  is chosen as one minute's measurement. Then, the rest measurement is divided into five groups and the correction times in MCFC are also five. Fig. 9(a)-(c) show the voltage and

OCV prediction results after charging condition. It is shown in Fig. 9(a)-(c) that the voltage shapes under various SOC levels are not exactly the same during the relaxation period. However, it is clearly seen from the partial enlarged figure of Fig. 9(a)-(c) that the OCV prediction with MCFC is approaching the reference at all SOC levels (5%, 50%, and 100%). At 100% SOC, the OCV prediction error is only 2.4 mV when uses the MCFC, while the OCV prediction errors in DCF and CFC are 158 mV and 30 mV respectively.

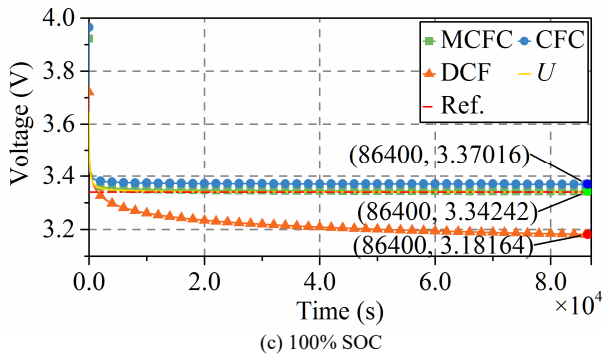
Fig. 9(d)-(f) shows the OCV prediction results in different discharging conditions. Similar to the previous case, the measurement during the first 15 minutes is used to predict the OCV. In Fig. 9(d)-(f), the performance of MCFC under various SOC levels obtains the best accuracy. In the case of 0% SOC in Fig. 9(d), the prediction error of the MCFC is only 3.97 mV, while the errors of the other two methods are almost 33 mV. MCFC shows the best OCV prediction accuracy at 50% SOC in Fig. 9(e). All the three methods are able to accurately predict the OCV at 95% SOC (Fig. 9(f)). The above experiments have proved that the MCFC has the capability of guaranteeing an accurate OCV prediction in both charging and discharging conditions.



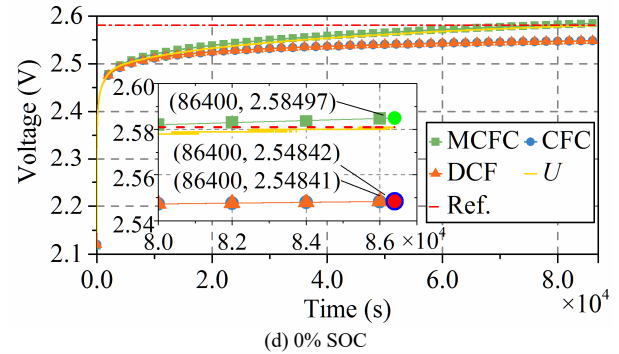
(a) 5% SOC



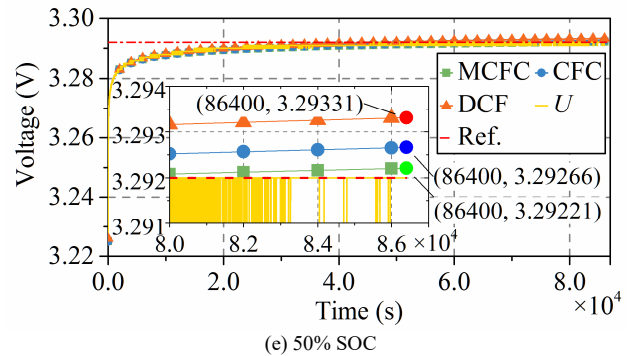
(b) 50% SOC



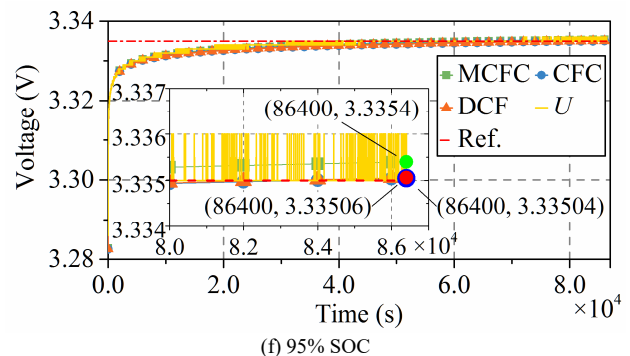
(c) 100% SOC



(d) 0% SOC



(e) 50% SOC



(f) 95% SOC

Fig. 9. Voltage prediction: (a), (b), (c) after charging condition; (d), (e), (f) after discharging condition.

### B. Validation with Different SOC levels

OCV not only varies with the charging and discharging conditions but also with the SOC levels. Therefore, the voltage variations under diverse SOC levels are measured to validate the proposed method. For the purpose of further validating the ability of OCV prediction, the LFP battery is tested from SOC=10% to SOC=90% with 10% interval and the voltage measurement during 4 hours' relaxation time is collected for validating the methods. The LFP battery is tested in the same condition as in Section. IV.A, which means the ambient temperature is also set to 25 °C and the sampling time is 1 second. Five minutes' measured data during the relaxation period is used to predict the voltage at 4 hours' relaxation time in both charging and discharging conditions. In MCFC, the measurement is divided into five groups with identical length, which means  $L_w$  contains only one minute's measurement and the correction times  $M$  are four. It is obvious in Fig. 10 that MCFC receives the best accuracy of the three methods, the absolute error of which is much lower than DCF and CFC in all the conditions.

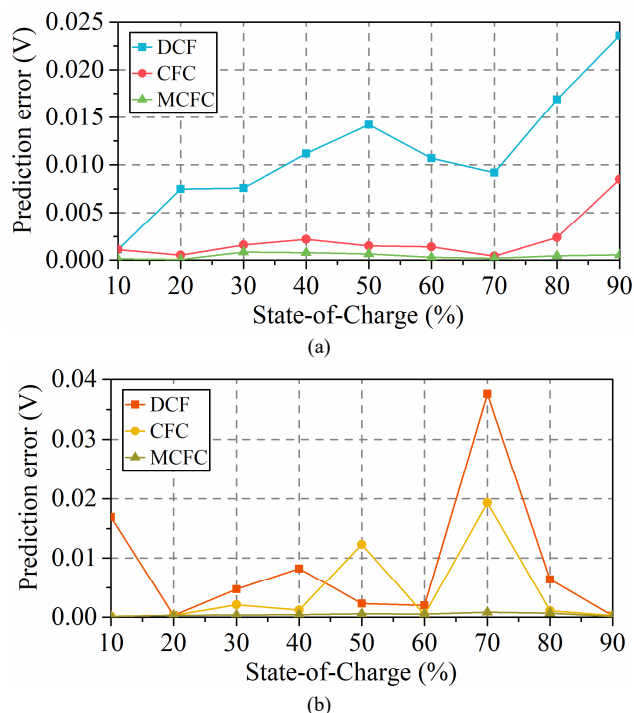


Fig. 10. Absolute error of the three methods in OCV prediction: (a) after charging condition; (b) after discharging condition.

The absolute error of OCV prediction using MCFC is less than 1 mV for all the SOCs, while the absolute errors of OCV prediction using the other two methods are much larger. Although all the methods are able to predict the OCV accurately at 20% and 90% SOC in the discharging condition, MCFC guarantees a better accuracy ( $< 1\text{mV}$ ) in diverse SOCs. The extended experiment has also proven that MCFC has the capability of accurately and rapidly predicting the OCV in various conditions. It is known that a small deviation of the curve fitting in the beginning of the relaxation period leads to a large error in the final OCV prediction. Compared with DCF and CFC, the multiple correction structure in MCFC can effectively reduce the sensitivity of the OCV prediction to the measurement error and the voltage shape at different SOCs.

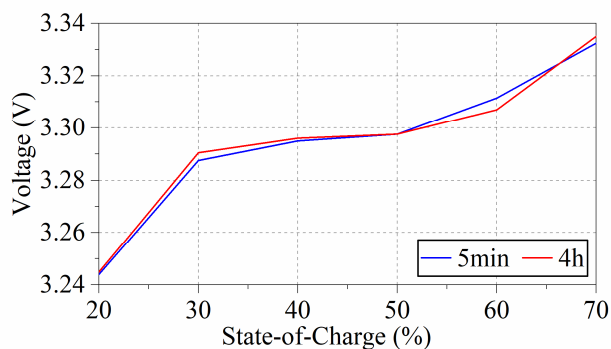


Fig. 11. OCV-SOC curve of the LFP battery

One possible usage of the proposed method is to construct the OCV-SOC characteristic of the battery. Since the LFP battery has a flat OCV-SOC curve, accurate OCV is extremely useful for the LFP battery based applications. The method in [30] calculates the average voltage between charge and

discharge within hours' relaxation time. Fig.11 shows a comparison of the average voltage method using 5 minutes' and 4 hours' relaxation time. The difference of the two average voltage is clearly seen from the Fig. 11. According to the OCV prediction results in Fig. 10, the proposed method using 5 minutes' measurement can obtain almost the same OCV-SOC curve as the average voltage method using 4 hours' relaxation time. Therefore, the time efficiency of the OCV measurement is improved by the proposed method.

## V. CONCLUSION

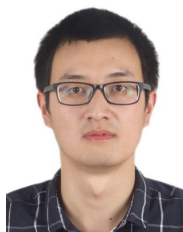
A novel multiple correction structure for fast OCV prediction of Li-ion battery is proposed in this paper, which obtains an accurate OCV in very short relaxation time. By analyzing the shape of the terminal voltage during the battery relaxation time, the efficiency of the traditional curve fitting method is significantly improved by adding a constraint to the power function. After investigating the shape of the prediction error in the preliminary curve fitting with constraint, a novel multiple correction approach is proposed to further improve the OCV prediction accuracy with even shorter relaxation time. Additionally, the proposed method does not require any previous knowledge of the electrochemistry, which can be easily used for different battery chemistries. Three methods (DCF, CFC and MCFC) have been proposed and compared in the experiments. MCFC shows the best OCV prediction accuracy (less than 1mV OCV estimation error with only 5 minutes' measurement and for a large SOC range (10%~90%)). Compared with DCF and CFC, the accuracy of the OCV prediction is effectively improved by MCFC. Therefore, MCFC is able to predict an accurate OCV with the voltage measurement in a very short relaxation time (less than 15 min).

## REFERENCES

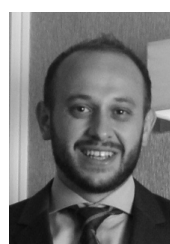
- [1] B. Diouf and R. Pode, "Potential of Lithium-ion Batteries in Renewable Energy," *Renewable Energy*, vol. 76, pp. 375–380, 2015.
- [2] X. Cao, Q. C. Zhong, Y. C. Qiao, and Z. Q. Deng, "Multilayer Modular Balancing Strategy for Individual Cells in a Battery Pack," *IEEE Trans. Energy Convers.*, vol. 33, no. 2, pp. 526–536, 2018.
- [3] D. Bazargan, B. Bahrani, and S. Filizadeh, "Reduced Capacitance Battery Storage DC-Link Voltage Regulation and Dynamic Improvement Using a Feed-Forward Control Strategy," *IEEE Trans. Energy Convers.*, p. 1, 2018.
- [4] M. Świerczyński *et al.*, "Field Experience from Li-Ion BESS Delivering Primary Frequency Regulation in the Danish Energy Market," *ECS Trans.*, vol. 61, no. 37, pp. 1–14, 2014.
- [5] Q. Jiang and H. Wang, "Two-Time-Scale Coordination Control for a Battery Energy Storage System to Mitigate Wind Power Fluctuations," *IEEE Trans. Energy Convers.*, vol. 28, no. 1, pp. 52–61, 2013.
- [6] A. Hentunen, T. Lehmuspelto, and J. Suomela, "Time-Domain Parameter Extraction Method for Thevenin-Equivalent Circuit Battery Models," *IEEE Trans. Energy Convers.*, vol. 29, no. 3, pp. 558–566, 2014.
- [7] J. Jaguemont, A. Nikolian, N. Omar, S. Goutam, J. Van Mierlo, and P. Van Den Bossche, "Development of a Two-Dimensional-Thermal Model of Three Battery Chemistries," *IEEE Trans. Energy Convers.*, vol. 32, no. 4, pp. 1447–1455, 2017.
- [8] K. Thirugnanam, J. T. P. Ezhil Reena, M. Singh, and P. Kumar, "Mathematical Modeling of Li-Ion Battery Using Genetic Algorithm Approach for V2G Applications," *IEEE Trans. Energy Convers.*, vol. 29, no. 2, pp. 332–343, 2014.
- [9] S. Tong, M. P. Klein, and J. W. Park, "On-line Optimization of Battery Open Circuit Voltage for Improved State-of-charge and State-of-health Estimation," *J. Power Sources*, vol. 293, pp. 416–428, 2015.



- [10] G. Ablay, "Online Condition Monitoring of Battery Systems With a Nonlinear Estimator," *IEEE Trans. Energy Convers.*, vol. 29, no. 1, pp. 232–239, 2014.
- [11] N. Mukherjee and D. De, "A New State-of-Charge Control Derivation Method for Hybrid Battery Type Integration," *IEEE Trans. Energy Convers.*, vol. 32, no. 3, pp. 866–875, 2017.
- [12] C. Weng, J. Sun, and H. Peng, "A Unified Open-circuit-voltage Model of Lithium-ion Batteries for State-of-charge Estimation and State-of-health Monitoring," *J. Power Sources*, vol. 258, pp. 228–237, 2014.
- [13] L. Lavigne, J. Sabatier, J. M. Francisco, F. Guillemard, and A. Noury, "Lithium-ion Open Circuit Voltage (OCV) Curve Modelling and Its Ageing Adjustment," *J. Power Sources*, vol. 324, pp. 694–703, 2016.
- [14] A. Farmann and D. U. Sauer, "A Study on the Dependency of the Open-circuit Voltage on Temperature and Actual Aging State of Lithium-ion batteries," *J. Power Sources*, vol. 347, no. Supplement C, pp. 1–13, 2017.
- [15] Y. Zheng *et al.*, "Cell State-of-charge Inconsistency Estimation for LiFePO<sub>4</sub> Battery Pack in Hybrid Electric Vehicles using Mean-difference Model," *Appl. Energy*, vol. 111, pp. 571–580, 2013.
- [16] C. Huang and L. Wang, "Gaussian Process Regression-based Modelling of Lithium-ion Battery Temperature-dependent Open-circuit-voltage," *Electron. Lett.*, Jul. 2017.
- [17] D.-I. Stroe, M. Swierczynski, A.-I. Stroe, and S. Knudsen Kær, "Generalized Characterization Methodology for Performance Modelling of Lithium-Ion Batteries," *Batteries*, vol. 2, no. 4, p. 37, 2016.
- [18] J. Meng *et al.*, "An Overview and Comparison of Online Implementable SOC Estimation Methods for Lithium-Ion Battery," *IEEE Trans. on Ind. Appl.*, 2018, vol. 54, no. 2, pp. 1583–1591.
- [19] M. A. Roscher, J. Assfalg, and O. S. Bohlen, "Detection of Utilizable Capacity Deterioration in Battery Systems," *IEEE Trans. Veh. Technol.*, vol. 60, no. 1, pp. 98–103, 2011.
- [20] Y.-S. Lee, M. Liu, C.-C. Sun, and M.-W. Cheng, "State-of-charge Estimation with Aging Effect and Correction for Lithium-ion Battery," *IET Electr. Syst. Transp.*, vol. 5, no. 2, pp. 70–76, 2015.
- [21] S. Nejad, D. T. Gladwin, and D. A. Stone, "A Systematic Review of Lumped-parameter Equivalent Circuit Models for Real-time Estimation of Lithium-ion Battery States," *Journal of Power Sources*, vol. 316, pp. 183–196, 2016.
- [22] T. Mesbahi, N. Rizoug, P. Bartholomeus, R. Sadoun, Fouad khenfri, and P. LE MOIGNE, "Dynamic Model of Li-Ion Batteries Incorporating Electrothermal and Ageing Aspects for Electric Vehicle Applications," *IEEE Trans. Ind. Electron.*, pp. 1–1, 2017.
- [23] P. Malysz, J. Ye, R. Gu, H. Yang, and A. Emadi, "Battery State-of-Power Peak Current Calculation and Verification using an Asymmetric Parameter Equivalent Circuit Model," *IEEE Trans. Veh. Technol.*, vol. 65, no. 6, pp. 4512–4522, 2016.
- [24] H. Hongwen, X. Rui, Z. Xiaowei, S. Fengchun, and F. JinXin, "State-of-Charge Estimation of the Lithium-Ion Battery Using an Adaptive Extended Kalman Filter Based on an Improved Thevenin Model," *Veh. Technol. IEEE Trans.*, vol. 60, no. 4, pp. 1461–1469, 2011.
- [25] R. Xiong, Q. Yu, L. Y. Wang, and C. Lin, "A Novel Method to Obtain the Open Circuit Voltage for the State of Charge of Lithium-ion Batteries in Electric Vehicles by using H Infinity Filter," *Applied Energy*, 2017.
- [26] M. Durbary, V. Svoboda, R. Hwu, and B. Y. Liaw, "Capacity Loss in Rechargeable Lithium Cells during Cycle Life Testing: The Importance of Determining State-of-charge," *J. Power Sources*, vol. 174, no. 2, pp. 1121–1125, 2007.
- [27] Z. Chen, Y. Fu, and C. C. Mi, "State of Charge Estimation of Lithium-Ion Batteries in Electric Drive Vehicles Using Extended Kalman Filtering," *IEEE Trans. Veh. Technol.*, vol. 62, no. 3, pp. 1020–1030, 2013.
- [28] C. R. Birkel, E. McTurk, M. R. Roberts, P. G. Bruce, and D. A. Howey, "A Parametric Open Circuit Voltage Model for Lithium Ion Batteries," *J. Electrochem. Soc.*, vol. 162, no. 12, pp. A2271–A2280, 2015.
- [29] S. J. Moura, "Estimation and Control of Battery Electrochemistry Models: A Tutorial," in *Proceedings of the IEEE Conference on Decision and Control*, 2015, vol. 54rd IEEE, pp. 3906–3912.
- [30] B. Pattipati, B. Balasingam, G. V. Avvari, K. R. Pattipati, and Y. Bar-Shalom, "Open Circuit Voltage Characterization of Lithium-ion Batteries," *J. Power Sources*, vol. 269, pp. 317–333, 2014.
- [31] F. Kazhamiaka, S. Keshav, C. Rosenberg, and K. H. Pettinger, "Simple Spec-Based Modelling of Lithium-Ion Batteries," *IEEE Trans. Energy Convers.*, p. 1, 2018.
- [32] A. B. Khan and W. Choi, "Optimal Charge Pattern for the High Performance Multi-Stage Constant Current Charge Method for the Li-ion Batteries," *IEEE Trans. Energy Convers.*, p. 1, 2018.
- [33] R. D'Agostino, L. Baumann, A. Damiano, and E. Boggasch, "A Vanadium-Redox-Flow-Battery Model for Evaluation of Distributed Storage Implementation in Residential Energy Systems," *IEEE Trans. Energy Convers.*, vol. 30, no. 2, pp. 421–430, 2015.
- [34] H. Chaoui, A. El Mejdoubi, and H. Gualous, "Online Parameter Identification of Lithium-Ion Batteries with Surface Temperature Variations," *IEEE Trans. Veh. Technol.*, vol. 66, no. 3, pp. 2000–2009, 2017.
- [35] T. Kim, Y. Wang, Z. Sahinoglu, T. Wada, S. Hara, and W. Qiao, "A Rayleigh Quotient-Based Recursive Total-Least-Squares Online Maximum Capacity Estimation for Lithium-Ion Batteries," *IEEE Trans. Energy Convers.*, vol. 30, no. 3, pp. 842–851, 2015.
- [36] L. Pei, T. Wang, R. Lu, and C. Zhu, "Development of a Voltage Relaxation Model for Rapid Open-circuit Voltage Prediction in Lithium-ion Batteries," *J. Power Sources*, vol. 253, pp. 412–418, 2014.
- [37] A. Li, S. Pelissier, P. Venet, and P. Gyan, "Fast Characterization Method for Modeling Battery Relaxation Voltage," *Batteries*, vol. 2, no. 2, p. 7, 2016.
- [38] M. Petzl and M. A. Danzer, "Advancements in OCV Measurement and Analysis for Lithium-ion Batteries," *IEEE Trans. Energy Convers.*, vol. 28, no. 3, pp. 675–681, 2013.
- [39] J. Meng, G. Luo, and F. Gao, "Lithium Polymer Battery State-of-Charge Estimation Based on Adaptive Unscented Kalman Filter and Support Vector Machine," *IEEE Trans. Power Electron.*, vol. 31, no. 3, pp. 2226–2238, 2016.
- [40] L. Pei, C. Zhu, and R. Lu, "Relaxation Model of the Open-circuit Voltage for State-of-charge Estimation in Lithium-ion Batteries," *IET Electr. Syst. Transp.*, vol. 3, no. 4, pp. 112–117, 2013.
- [41] V. Pop, H. J. Bergveld, D. Danilov, P. P. L. Regtien, and P. H. L. Notten, Eds., "Methods for Measuring and Modelling a Battery's Electro-Motive Force BT - Battery Management Systems: Accurate State-of-Charge Indication for Battery-Powered Applications," Dordrecht: Springer Netherlands, 2008, pp. 63–94.
- [42] D. Bolmatov, V. V. Brazhkin, and K. Trachenko, "Thermodynamic Behaviour of Supercritical Matter," *Nat. Commun.*, vol. 4, 2013.



**Jinhao Meng (S'14)** received the M.S. degree in control theory and control engineering from Northwestern Polytechnical University (NPU), Xi'an, China, in 2013, where he is currently working toward the Ph.D. degree in electrical engineering. He is supported by the China Scholarship Council as a joint Ph.D. student with the Department of Energy Technology, Aalborg University, Aalborg, Denmark, from 2016 to 2018.



**Daniel-Ioan Stroe (M'11)** received the Dipl.-Ing. degree in automatics from Transilvania University of Brasov, Romania, in 2008, and M.Sc. degree in wind power systems from Aalborg University, Aalborg, Denmark, in 2010. He has been with Aalborg University since 2010, from where he obtained his Ph.D. degree in lifetime modelling of Lithium-ion batteries in 2014.

Currently, he is an Associate Professor with the Department of Energy Technology, where he leads the Battery Storage Systems research programme and the Battery Systems Testing Lab. He was a Visiting Researcher with RWTH Aachen, Germany, in 2013. He has co-authored over 90 journal and conference papers in various battery-related topics. His current research interests are in the area of energy storage systems for

grid and e-mobility, Lithium-based batteries testing, modelling, diagnostics and their lifetime estimation.



**Mattia Ricco** (M'16) received the master's degree (cum laude) in electronic engineering from the University of Salerno, Fisciano, Italy, in 2011, and the Ph.D. degrees in electrical and electronic engineering from the University of Cergy-Pontoise, Cergy-Pontoise, France, and in information engineering from the University of Salerno, in 2015.

Since September 2015, he has been a Postdoctoral Research Fellow with the Department of Energy Technology at Aalborg University, Aalborg, Denmark. His main research interests include FPGA-based controllers, active battery management system, digital control of modular multilevel converters and identification algorithms for power electronics and photovoltaic systems.



**Guangzhao Luo** (M'08) received the M.S. and Ph.D. degrees in electrical engineering from Northwestern Polytechnical University (NPU), Xi'an, China, in 1998 and 2003, respectively.

From 2003 to 2004, he was a Postdoctoral Research at the University of Federal Defense, Munich, Germany. He is currently a Professor with NPU. He is the Vice Director of the Rare Earth Permanent Magnet (REPM) Electric Machine and Control Engineering Center, Shaanxi Province. His research interests include advance control theory of permanent magnet electrical machine, high performance control technology of permanent magnet synchronous motor for electric traction and electric vehicle, real-time simulation technology for electrical drive system, and intelligence control of new energy conversion. Dr. Luo received the Second Prize from the China National Defense Science and Technology Progress Award in 1995 and 2011.



**Maciej Swierczynski** (M'14) received the M. Tech degree from AGH University of Science and Technology, Poland in 2007 in Computer Engineering for Industrial Applications, and from Aalborg University, Denmark in 2009 in Power Electronics and Drives. In 2012, he completed his Ph.D. at Aalborg University, Denmark. Later, he worked as

a postdoctoral researcher and Associate Professor at Aalborg University in 2013-2017.

In 2018, he moved to the industry where he is currently working in Lithium Balance A/S as R&D specialist. His area of research is in battery technologies for renewables, EV and residential applications, battery management, testing, modelling and lifetime analyses.



**Remus Teodorescu** (F'12) received the Dipl.-Ing. degree in electrical engineering from the Polytechnical University of Bucharest, Bucharest, Romania, in 1989, and the Ph.D. degree in power electronics from the University of Galati, Galati, Romania, in 1994.

In 1998, he joined the Power Electronics Section, Department of Energy Technology, Aalborg University, Aalborg, Denmark, where he is currently a Full Professor. Since 2013, he has been a Visiting Professor with Chalmers University. His research interests include design and control of grid-connected converters for photovoltaic and wind power systems, high voltage dc/flexible ac transmission systems based on modular multilevel converters, and storage systems based on Li-ion battery technology including modular converters and active battery management systems.